



Morphometric and Microstructural Characteristics of the Brain in Patients with Temporal Lobe Epilepsy

Marina Yu. Maximova, Anna D. Shitova, Marina V. Krotenkova, Anastasia N. Sergeeva

Russian Center of Neurology and Neurosciences, Moscow, Russia

Abstract

Introduction. The study of morphometric and microstructural characteristics of the brain in patients with temporal lobe epilepsy (TLE) represents one of the most rapidly advancing areas of neuroimaging research.

Study aim: To quantitatively assess changes in morphometric and microstructural parameters of gray and white matter in the brains of patients with TLE.

Materials and methods. The study included 55 subjects (29 patients with temporal lobe epilepsy and 26 healthy controls) aged 22–64 years. All patients underwent brain MRI according to an epilepsy protocol and diffusion MRI (3 Tesla). Voxel-based morphometry was performed using the CAT12 module in MATLAB 2018. Modeling of 32 white matter tracts was conducted automatically in DSI Studio 2022 using the HCP842 atlas-based algorithm.

Results. Patients with TLE showed significant gray matter volume reduction in 54 regions and white matter volume reduction in 23 regions. Conversely, white matter volume increase was observed in 6 regions. Subgroup analysis of different structural abnormalities (hippocampal sclerosis, focal cortical dysplasia, low-grade glioneuronal tumor, cavernoma, encephalocele) revealed gray matter volume increase in 9 regions and white matter increase in 1 region. Additionally, white matter volume increase was documented in 3 regions in patients with bitemporal discharges and in 2 regions with hippocampal sclerosis. Microstructural changes were detected bilaterally – both ipsilateral and contralateral to the epileptogenic focus. Some changes indicated enhanced microstructural integrity and compaction of myelin fibers.

Conclusion. Patients with TLE exhibit not only morphometric and microstructural signs of degenerative changes in cerebral gray and white matter, but also markers of compensatory neuroplastic mechanism activation.

Keywords: temporal lobe epilepsy; hippocampal sclerosis; white matter; epileptogenic network; voxel-based morphometry; tractography

Ethics approval. All patients provided their written informed consent to participate in the study. The study protocol was approved by the Local Ethics Committee of the Russian Center of Neurology and Neurosciences (Protocol No. 2-5/25 dated February 17, 2025).

Source of funding. The study was performed as part of the state assignment of the Russian Center of Neurology and Neurosciences (No. 123120100066-8).

Conflict of interest. The authors declare no apparent or potential conflicts of interest related to the publication of this article.

For correspondence: 80, Volokolamskoe shosse, Moscow, Russia, 125367. Russian Center of Neurology and Neurosciences. E-mail: ncnmaximova@mail.ru. Marina Yu. Maximova.

For citation: Maximova M.Yu., Shitova A.D., Krotenkova M.V., Sergeeva A.N. Morphometric and microstructural characteristics of the brain in patients with temporal lobe epilepsy. *Annals of Clinical and Experimental Neurology*. 2026;20(1):27–38.

DOI: <https://doi.org/10.17816/ACEN.1473>

EDN: <https://elibrary.ru/FHYRGW>

Received 15.01.2026 / Accepted 30.01.2026 / Published 30.03.2026

Исследование морфометрических и микроструктурных характеристик головного мозга у пациентов с височной эпилепсией

М.Ю. Максимова, А.Д. Шитова, М.В. Кротенкова, А.Н. Сергеева

Российский центр неврологии и нейронаук, Москва, Россия

Аннотация

Введение. Исследование морфометрических и микроструктурных характеристик мозга у пациентов с височной эпилепсией (ВЭ) представляет собой одно из наиболее активно развивающихся направлений в области нейровизуализации.

Цель исследования: количественно оценить изменения морфометрических и микроструктурных параметров серого и белого вещества головного мозга у пациентов с ВЭ.

Материалы и методы. В исследование были включены 29 пациентов с ВЭ и 26 здоровых лиц в возрасте 22–64 лет. Всем пациентам были проведены МРТ головного мозга по эпилептологическому протоколу и диффузионная МРТ (3 Тл). Для воксель-ориентированной морфометрии использовали модуль CAT12 в среде MATLAB 2018. Моделирование 32 трактов белого вещества выполняли в автоматическом режиме в программе «DSI Studio 2022» с использованием алгоритма, основанного на атласе HCP842.

Результаты. У пациентов с ВЭ обнаружено значительное снижение объёма серого вещества в 54 областях и объёма белого вещества – в 23 областях. При этом в 6 областях наблюдалось увеличение объёма белого вещества. Анализ подгрупп с различными видами структурной патологии (склероз гиппокампа, фокальная корковая дисплазия, глионейронная опухоль низкой степени злокачественности, кавернома, энцефалоцеле) показал увеличение объёма серого вещества в 9 областях и белого вещества – в 1 области. Кроме того, увеличение объёма белого вещества было зафиксировано в 3 областях у пациентов с битемпоральными разрядами и в 2 областях при склерозе гиппокампа. Микроструктурные изменения выявлены в обоих полушариях – как на стороне эпилептогенного очага, так и на противоположной. Часть этих изменений указывала на повышение микроструктурной целостности и уплотнение миелиновых волокон.

Заключение. У пациентов с ВЭ выявляются не только морфометрические и микроструктурные признаки дегенеративных изменений серого и белого вещества головного мозга, но и маркеры активации компенсаторных нейропластических механизмов.

Ключевые слова: височная эпилепсия; склероз гиппокампа; белое вещество; эпилептогенная сеть; воксель-ориентированная морфометрия; трактография

Этическое утверждение. Исследование проводилось при добровольном информированном письменном согласии пациентов. Протокол исследования одобрен локальным этическим комитетом Российского центра неврологии и нейронаук (протокол № 2-5/25 от 17.02.2025).

Источник финансирования. Работа выполнена в рамках государственного задания Российского центра неврологии и нейронаук (№ 123120100066-8).

Конфликт интересов. Авторы заявляют об отсутствии явных и потенциальных конфликтов интересов, связанных с публикацией настоящей статьи.

Адрес для корреспонденции: 125367, Россия, Москва, Волоколамское ш., д. 80. Российский центр неврологии и нейронаук. E-mail: ncnmaximova@mail.ru. Максимова М.Ю.

Для цитирования: Максимова М.Ю., Шитова А.Д., Кротенкова М.В., Сергеева А.Н. Исследование морфометрических и микроструктурных характеристик головного мозга у пациентов с височной эпилепсией. *Анналы клинической и экспериментальной неврологии.* 2026;20(1):27–38.

DOI: <https://doi.org/10.17816/ACEN.1473>

EDN: <https://elibrary.ru/FHYRGW>

Поступила 15.01.2026 / Принята в печать 30.01.2026 / Опубликовано 30.03.2026

Introduction

Temporal lobe epilepsy (TLE) is the most common form of focal epilepsy, often characterized by a drug resistance [1]. Traditionally, hippocampal sclerosis is considered the primary structural substrate of TLE, detected in 69.3% of cases [2]. However, cohort study results demonstrate significant variability in structural abnormalities. For instance, in the

study by N. Hainc et al. hippocampal sclerosis was diagnosed on magnetic resonance imaging (MRI) in only 17.9% patients with drug-resistant TLE, Dual abnormality was detected in 8.7%, and no structural changes were diagnosed in 35.5% of patients (MRI-negative cases) [1].

Despite isolated cases of successful surgical treatment in patients with MRI-negative focal epilepsy and histologically

verified diagnosis [1, 3], the rate of postoperative seizure freedom in this group remains significantly lower than in patients with MRI-detectable structural changes [4]. The prognosis for both conservative and surgical treatment further worsens with bitemporal epileptiform activity, which occurs in 15% of cases [2]. Consequently, the search for neuroimaging biomarkers for precise localization and lateralization of the epileptogenic focus represents an urgent scientific and practical challenge. Solving this challenge could enhance the efficacy of surgical treatment.

In recent years, the network model of epileptogenesis has been actively developing. According to this concept, pathological activity is generated not by a single focus but by a distributed neural network involving various regions of the brain. Neurons in the cerebral cortex, subcortical structures, brainstem, and cerebellum may be involved. Thus, pathological changes extend not only to areas adjacent to the epileptogenic focus but also to functionally connected remote brain regions united into a single epileptic network.

The white matter of the brain forms the structural framework of neural networks, including those involved in epileptic activity. Studying its alterations in epilepsy is crucial for understanding the structural basis of this disease. The most informative method for *in vivo* visualization of white matter microstructure is diffusion tensor MRI.

Study aim: to quantitatively assess changes in morphometric and microstructural parameters of gray and white matter in the brains of patients with TLE.

Materials and Methods

A cohort cross-sectional study was conducted based at the 2nd Neurology department of the Russian Center of Neurology and Neurosciences during 2025.

The study included 55 subjects. The main group comprised 29 patients with TLE (10 men and 19 women aged 22–64 years; mean age 38.9 years), whose diagnosis was confirmed by brain MRI using an epileptological protocol and 24-hour video-electroencephalographic (EEG) monitoring. The control group included 26 healthy volunteers without epilepsy or other neurological and psychiatric diseases, matched to the main group by sex and age (8 men and 18 women aged 20–51 years; mean age 30 years).

Prior to inclusion in the study, written informed consent was obtained from each participant. The study protocol was approved by the Local Ethics Committee of the Russian Center of Neurology and Neurosciences (Protocol No. 2-5/25 dated February 17, 2025).

Exclusion criteria: history of cerebrovascular and inflammatory brain diseases, generalized epilepsy, psychogenic non-epileptic seizures. These conditions were excluded following a comprehensive analysis of medical history, neurological examination, and diagnostic tests.

Lateralization of the primary epileptogenic focus required for subsequent assessment of ipsi- and contralateral

changes was performed considering EEG discharge patterns: monotemporal discharges were lateralized according to the hemisphere of epileptiform activity registration on EEG; bitemporal discharges were lateralized based on ictal semiology and structural MRI changes.

MRI Brain Image Registration

Brain MRI images of all study participants were acquired simultaneously on a Siemens Magnetom Prisma scanner (Siemens AG) with a magnetic field strength of 3 T. The scanning protocol adhered to the epileptological standard and included standard clinical sequences (2D T2-weighted imaging, 3D T2-FLAIR, SWI, DWI) and additional sequences of the epileptological protocol (3D T2-FLAIR, 3D MP2RAGE, 2D T2-weighted imaging), acquired parallel and perpendicular to the hippocampal axis. A single-shot spin-echo sequence was used to acquire diffusion-weighted data with the following parameters: isotropic voxel size of 2 mm, TR/TE = 12,600/115 ms, and a matrix of 100 × 100 pixels. Diffusion weighting was applied for 3 b-values (b = 0, 1000, 2500 s/mm²) along 64 diffusion gradient directions.

On T1-weighted images, intensity inhomogeneity correction, intensity normalization, and linear registration to the symmetric standard MNI ICBM152 space were performed.

Processing of diffusion tensor MRI data included correction for artifacts due to patient motion and distortions from eddy currents using the eddy tool from the FSL software package.

MRI Postprocessing

Voxel-based morphometry was performed using SPM12 (Statistical Parametric Mapping)¹ with the CAT12 morphometric module in the MATLAB environment². The Neuroinformatics atlas (<https://neuroinformatics.com/Seg/>) was used for automated segmentation of brain structures.

Tractography and diffusion parameter analysis were performed using DSI Studio software (Chen version dated 01.08.2022, <https://dsi-studio.labsolver.org/>). Preprocessing of diffusion data included normalization to the standard MNI space. Tractography was performed automatically using an algorithm based on the HCP842 tract atlas [5], integrated into the ICBM152 adult template. Anatomical accuracy of the identified tracts was additionally verified through visual assessment. Tractometry (a quantitative analysis) was performed for each identified tract, calculating mean values of key diffusion parameters: fractional anisotropy (FA), mean diffusivity (MD), axial diffusivity (AD), and radial diffusivity (RD).

Quality assessment of brain MRI results according to the epileptological protocol was performed at the patient selection stage, strictly adhering to the inclusion and exclusion criteria. The study included only patients with MRI-negative epilepsy,

¹URL: <https://www.fil.ion.ucl.ac.uk/spm/software/spm12/>

²Gaser C, Dahnke R, Thompson PM, Kurth F, Luders E, Alzheimer's Disease Neuroimaging Initiative (2024). CAT: a computational anatomy toolbox for the analysis of structural MRI data. *Gigascience* 13, giae049. URL: <https://neuro-jena.github.io/cat12-help/#cite>

mesial temporal lobe epilepsy associated with hippocampal sclerosis, and non-hippocampal structural epilepsy. During MRI postprocessing, the segmentation results obtained using morphometric and tractographic atlases were visually evaluated using visualization tools in 3D Slicer, FreeSurfer (FreeView), and DSI Studio with the participation of a neurologist and a radiologist. At this stage, the segmentation results corresponded to the anatomical boundaries of brain structures without displacement, and consequently, no cases were excluded during MRI postprocessing.

Statistical Analysis

Statistical analysis was performed using SPSS 26.0 software (IBM). Due to the small sample size and deviation from normal distribution, non-parametric methods were applied for analysis. Data are presented as median (Me) and interquartile range [Q₁; Q₃]. Quantitative variables between groups were compared using the Mann–Whitney U test. Differences were considered statistically significant at $p < 0.05$.

Results

The general characteristics of the patients are presented in the Table 1. Distribution of TLE patients based on MRI findings was as follows:

- Signs of hippocampal sclerosis – 10 patients (characterized by hippocampal volume reduction and hyperintense signal on T2 and T2-FLAIR sequences);
- Other structural (non-hippocampal) abnormalities – 7 patients. This group included cases of focal cortical dysplasia (2), temporal lobe cavernoma (2), low-grade temporal lobe glioneuronal tumor (2), and left temporal pole encephalocele (1);
- MRI-negative TLE – 12 patients (no evidence of structural abnormality on MRI).

Bitemporal epileptiform discharges were recorded in 8 patients, 4 of whom had the MRI-negative form.

The mean TLE duration at the time of the study was 16.8 years (range 1–37 years). The mean duration of pharmacotherapy was 150.9 months (range 6–444 months). Drug-resistant TLE was observed in 14 patients, including 5 patients with the MRI-negative form and 6 patients with hippocampal sclerosis.

Table 1. Characteristic of the main group

Condition	Sex	Age at onset, years	Age during the study, years	Pharmacotherapy duration, months	Bitemporal epileptiform discharges	Drug-resistance	Presence of bilateral tonic-clonic seizures
Hippocampal sclerosis	Male	5–58	22–62	13–44	1	2	3
	Female	0–25	27–60	120–360	1	4	4
Structural (non-hippocampal) abnormalities	Male	5–58	22–62	13–444	2	2	2
	Female	0–32	22–60	0–360	0	2	5
MRI-negative epilepsy	Male	17–63	27–64	6–276	1	0	3
	Female	0–32	22–60	0–360	3	4	6

Voxel-Based Morphometry

The results of the analysis of morphometric parameters in the main patient group and in the healthy control group are presented in Table 2, Table 3, and Fig. 1.

The diagram was generated using 3D Slicer software with FreeSurfer_DKT. FreeSurfer's standard color map was used for anatomical region labeling.

Patients with TLE showed statistically significant reductions in gray matter volume in 54 regions and white matter volume in 23 regions compared to healthy controls. Gray matter atrophy predominantly localized ipsilateral to the primary epileptogenic focus (29 regions ipsilateral, 25 contralateral). In white matter, contralateral changes predominated (10 regions ipsilateral, 13 contralateral). Gray matter alterations involved both hemispheres, affecting temporal, frontal, occipital, parietal lobes, and insular cortex. The most pronounced volume reduction was observed in ipsilateral temporal and frontal cortex regions.

Bilateral changes involved key limbic structures (cingulate, orbitofrontal, entorhinal, and subcallosal cortices; nucleus accumbens), visual system (primary visual cortex, cuneus, lingual gyrus, occipital gyrus, fusiform gyrus, occipital pole), and motor systems (primary motor cortex, premotor cortex, supplementary motor area, medial prefrontal cortex).

Gray matter alterations in the brain exhibited clear lateralization. In the parietal lobe, contralateral changes were predominantly localized to somatosensory areas (postcentral gyrus, supramarginal gyrus, parietal operculum). Ipsilateral changes were detected in structures associated with visuospatial functions (entorhinal cortex, precuneus, supramarginal gyrus, angular gyrus). In the cerebellum, bilateral cortical volume reduction was observed, with contralateral reduction additionally noted in the cerebellar vermis lobules. Subcortical structures showed gray matter volume reduction (bilateral in caudate nucleus, ipsilateral in putamen and thalamus, contralateral in nucleus accumbens).

White matter volume reduction was detected in the ipsilateral cerebral hemisphere and contralateral cerebellar hemisphere. In most cases, alterations were localized to superficial white matter regions adjacent to pathologically altered cortical (gray matter)

Table 2. Regions of interest (ROIs) in gray matter with differences in morphometric parameters in patients with TLE compared to the healthy control group, median [Q₁; Q₃]

Brain structures	Main group	Comparison group	p
Ipsilateral side			
Caudate nucleus	2.75 [2.36; 2.83]	3.08 [2.80; 3.25]	0.001
Cerebellar hemisphere cortex	44.82 [41.75; 46.82]	49.09 [47.32; 53.47]	0.001
Hippocampus	2.83 [2.31; 3.27]	3.37 [3.12; 3.55]	0.002
Putamen	3.86 [3.64; 4.17]	4.17 [3.72; 4.58]	0.049
Thalamus	5.11 [4.73; 5.23]	5.62 [5.44; 5.86]	0.001
Anterior orbital gyrus	1.71 [1.49; 1.91]	2.03 [1.79; 2.19]	0.002
Angular gyrus	7.00 [6.42; 8.14]	8.96 [8.01; 9.75]	0.001
Primary visual cortex	2.51 [2.33; 2.85]	2.80 [2.46; 3.25]	0.049
Cuneus	3.58 [3.11; 3.98]	4.09 [3.66; 4.30]	0.006
Entorhinal cortex	2.26 [1.94; 2.44]	2.44 [2.31; 2.68]	0.013
Frontal operculum	1.49 [1.27; 1.63]	1.62 [1.56; 1.75]	0.016
Fusiform gyrus	7.28 [6.63; 7.75]	8.44 [8.02; 8.83]	0
Straight gyrus	2.50 [2.16; 2.68]	2.66 [2.49; 3.04]	0.025
Inferior occipital gyrus	4.91 [4.59; 5.62]	5.85 [5.30; 6.68]	0.001
Inferior temporal gyrus	11.53 [10.34; 12.83]	13.14 [12.15; 14.50]	0.005
Lingual gyrus	6.64 [5.94; 7.30]	7.52 [6.98; 8.13]	0.009
Lateral orbital gyrus	2.01 [1.88; 2.17]	2.19 [1.95; 2.48]	0.035
Medial segment of superior frontal gyrus	2.02 [1.84; 2.24]	2.24 [1.94; 2.37]	0.024
Medial segment of superior frontal gyrus	5.36 [4.95; 5.98]	6.57 [6.08; 7.38]	0
Middle temporal gyrus	11.94 [10.89; 13.45]	13.93 [12.73; 15.78]	0.004
Opercular part of inferior frontal gyrus	2.50 [2.33; 2.71]	2.80 [2.56; 3.18]	0.006
Precuneus	8.44 [7.39; 9.33]	10.02 [8.80; 10.66]	0.001
Posterior insula	1.81 [1.71; 1.89]	2.00 [1.80; 2.16]	0.008
Posterior orbital gyrus	2.79 [2.55; 2.93]	3.02 [2.89; 3.31]	0
Supplementary motor area	4.18 [3.94; 4.53]	4.66 [4.20; 5.13]	0.025
Supramarginal gyrus	6.32 [5.57; 6.98]	7.20 [6.69; 7.74]	0.006
Superior occipital gyrus	2.68 [2.41; 2.95]	3.37 [3.00; 3.69]	0
Superior temporal gyrus	5.67 [5.13; 6.21]	6.51 [5.89; 7.30]	0.003
Temporal pole	8.57 [7.74; 8.99]	9.74 [8.74; 10.35]	0.004
Contralateral side			
Nucleus accumbens	0.36 [0.33; 0.39]	0.43 [0.39; 0.47]	0
Cerebellar cortex	45.21 [40.72; 47.36]	49.33 [44.73; 52.12]	0.006
Putamen	3.83 [3.65; 4.17]	4.22 [3.89; 4.61]	0.032
Anterior cingulate cortex	3.28 [3.04; 3.71]	4.03 [3.67; 4.57]	0
Lateral orbital gyrus	1.96 [1.85; 2.20]	2.22 [2.12; 2.53]	0.001
Middle frontal gyrus	14.37 [12.58; 15.69]	16.22 [14.31; 17.48]	0.034
Middle occipital gyrus	4.17 [3.75; 4.60]	5.07 [4.55; 5.30]	0.001
Middle orbital gyrus	4.75 [4.01; 5.10]	5.14 [4.70; 5.42]	0.006
Occipital pole	3.24 [2.95; 3.68]	3.95 [3.31; 4.30]	0.02
Fusiform gyrus	3.18 [2.88; 3.46]	3.40 [3.20; 3.96]	0.025
Orbital part of inferior frontal gyrus	1.23 [1.09; 1.36]	1.38 [1.18; 1.49]	0.012
Posterior cingulate gyrus	3.05 [2.78; 3.38]	4.05 [3.43; 4.33]	0
Precuneus	8.34 [7.54; 9.27]	9.73 [8.69; 10.55]	0.004
Parietal operculum	1.55 [1.28; 1.81]	1.98 [1.59; 2.13]	0.009
Postcentral gyrus	7.49 [6.78; 8.03]	9.47 [8.65; 10.18]	0
Posterior orbital gyrus	2.78 [2.45; 3.11]	3.16 [2.95; 3.38]	0.004
Anterior part of superior temporal gyrus	1.52 [1.36; 1.58]	1.62 [1.47; 1.75]	0.011
Precentral gyrus	9.94 [9.34; 10.39]	11.02 [9.97; 11.67]	0.009
Subcallosal area	1.33 [1.24; 1.51]	1.52 [1.43; 1.63]	0.006
Supplementary motor area	4.08 [3.81; 4.56]	4.69 [4.28; 5.09]	0.009
Supramarginal gyrus	6.12 [5.76; 7.00]	7.49 [6.44; 7.85]	0.004
Superior parietal lobule	7.84 [7.40; 8.59]	9.08 [8.33; 9.43]	0.001
Heschl's gyrus	0.97 [0.89; 1.14]	1.11 [0.94; 1.30]	0.038
Cortex of cerebellar vermis lobules VI-VII	1.75 [1.56; 1.91]	1.99 [1.83; 2.14]	0.004
Cortex of cerebellar vermis lobules VIII-X	2.25 [2.07; 2.38]	2.43 [2.25; 2.64]	0.005

Table 3. Regions of interest (ROIs) in white matter with differences in morphometric parameters in patients with TLE compared to the healthy control group, median [Q₁; Q₃]

Brain structures	Main group	Comparison group	p
Ipsilateral side			
White matter of the cerebral hemisphere	172.88 [154.86; 179.94]	179.39 [174.29; 192.50]	0.016
Anterior cingulate gyrus	0.43 [0.30; 0.56]*	0.31 [0.25; 0.41]	0.021
Anterior orbital gyrus	0.22 [0.18; 0.27]	0.26 [0.21; 0.29]	0.043
Angular gyrus	1.43 [1.35; 1.66]	1.70 [1.53; 1.95]	0.032
Frontal operculum	0.13 [0.10; 0.15]	0.16 [0.14; 0.20]	0.004
Fusiform gyrus	1.08 [0.94; 1.26]	1.39 [1.12; 1.46]	0.022
Straight gyrus	0.40 [0.32; 0.49]	0.53 [0.42; 0.59]	0.012
Middle occipital gyrus	0.88 [0.73; 1.06]*	0.72 [0.65; 0.82]	0.004
Medial segment of superior frontal gyrus	0.77 [0.72; 0.86]	0.89 [0.80; 1.04]	0.011
Occipital pole	0.65 [0.55; 0.78]*	0.55 [0.51; 0.65]	0.016
Precuneus	1.51 [1.22; 1.61]	1.66 [1.57; 1.83]	0.019
Posterior insula	0.09 [0.08; 0.12]	0.13 [0.12; 0.14]	0.008
Superior occipital gyrus	0.65 [0.59; 0.71]	0.75 [0.64; 0.85]	0
Heschl's gyrus	0.22 [0.11; 0.29]*	0.14 [0.10; 0.16]	0.028
Contralateral side			
White matter of cerebellar hemisphere	10.55 [10.30; 11.30]	11.60 [10.73; 12.37]	0.009
Thalamus	2.14 [1.88; 2.38]	2.44 [2.26; 2.62]	0
Ventral forebrain	3.52 [3.37; 3.82]	3.82 [3.73; 4.01]	0.004
Anterior cingulate gyrus	0.41 [0.33; 0.48]	0.59 [0.49; 0.61]	0
Primary visual cortex	0.61 [0.52; 0.70]	0.70 [0.65; 0.82]	0.009
Straight gyrus	0.46 [0.36; 0.52]*	0.36 [0.32; 0.40]	0.011
Inferior occipital gyrus	1.23 [0.94; 1.40]	1.40 [1.20; 1.50]	0.029
Middle occipital gyrus	0.78 [0.66; 0.96]	0.93 [0.84; 1.06]	0.013
Middle orbital gyrus	0.64 [0.53; 0.74]	0.82 [0.74; 0.89]	0
Posterior cingulate gyrus	0.41 [0.37; 0.50]	0.51 [0.45; 0.56]	0.001
Parietal operculum	0.17 [0.14; 0.23]	0.25 [0.20; 0.28]	0.001
Postcentral gyrus	1.82 [1.59; 2.10]	2.12 [1.94; 2.27]	0.02
Supramarginal gyrus	1.29 [1.13; 1.50]	1.53 [1.29; 1.66]	0.032
Superior parietal lobule	1.95 [1.83; 2.17]	2.21 [2.01; 2.56]	0.008
Pars triangularis of inferior frontal gyrus	0.48 [0.42; 0.60]*	0.41 [0.38; 0.51]	0.042

Note: Here and in Tables 4–6: * measurement values in the main patient group are higher than in the healthy control group.

areas. The degree of white matter volume reduction was less pronounced compared to gray matter changes. Segmentation and volumetry of deep white matter regions were not performed due to lack of appropriate atlas in the software used.

Additionally, patients with epilepsy showed increased white matter volume in 6 brain regions compared to healthy controls. Four of these regions were ipsilateral to the epileptogenic focus (superficial white matter of occipital cortex, temporal cortex, and cingulate gyrus), while two were contralateral (straight gyrus and inferior frontal gyrus) (Table 3).

Comparative analysis of TLE patients groups selected according to clinical and morphological characteristics, i.e. patients with hippocampal sclerosis, other structural (non-hippocampal) abnormalities, drug resistance, and bitemporal discharges, revealed statistically significant differences in frontal/tem-

poral lobe, forebrain, and brainstem involvement (Table 4). Regarding parietal lobe, differences less frequently reached statistical significance and were less pronounced.

In cases of other (non-hippocampal) structural abnormalities, bilateral reduction of gray matter volume was noted in the ventral portions of the forebrain and brainstem. White matter volume reduction was bilateral in the medial part of the superior frontal gyrus and contralateral in the cerebellar hemisphere and cingulate gyrus. Combined reduction of both tissue types was observed in the brainstem.

In patients with MRI-detected structural abnormalities compared to those without pathological changes, increased gray matter volume was detected in 9 regions. These included 4 temporal cortex regions (ipsilaterally – middle temporal gyrus; contralaterally – temporal pole, middle temporal gyrus,

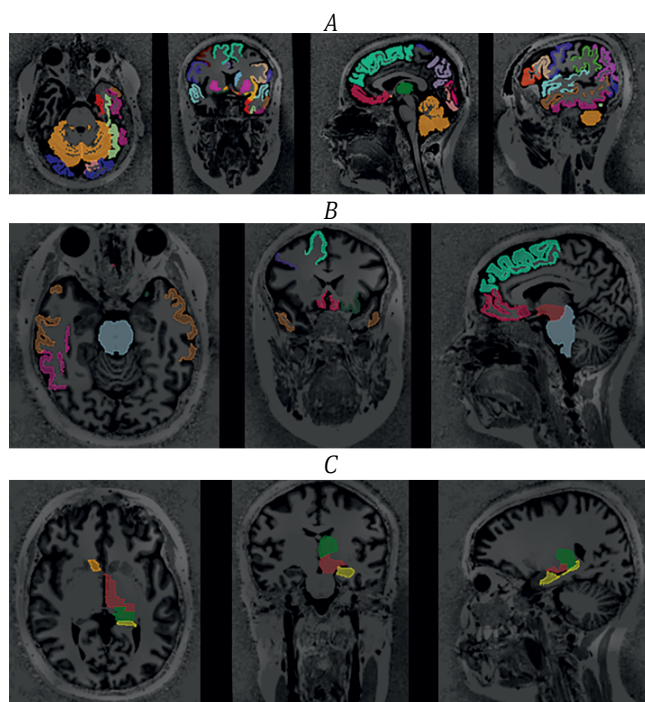


Fig. 1. Gray matter regions of interest (ROIs) showing differences between patients with temporal lobe epilepsy and healthy controls.

A – temporal lobe epilepsy; *B* – structural (non-hippocampal) abnormalities; *C* – hippocampal sclerosis.

and inferior temporal gyrus), 2 frontal cortex regions (medial frontal cortex and medial segment of superior frontal gyrus), as well as ipsilateral anterior cingulate gyrus and bilateral subcallosal area. White matter volume was increased in the anterior part of the insular lobe.

In hippocampal sclerosis, ipsilateral reduction of gray matter volume was noted in the ventral forebrain and thalamus, and of white matter – in the parahippocampal gyrus and planum temporale. Contralateral changes included gray matter reduction in the nucleus accumbens area and white matter reduction – in the orbital part of the inferior frontal gyrus and postcentral gyrus. Additionally, white matter volume increase was observed in 2 regions (ipsilateral planum temporale and contralateral postcentral gyrus).

Patients with drug-resistant TLE showed bilateral reduction of gray matter volume in the ventral forebrain. White matter changes were bilateral in the medial part of the precentral gyrus, with ipsilateral involvement in the medial postcentral gyrus and contralateral involvement in the parahippocampal gyrus.

Patients with bitemporal epileptiform discharges exhibited increased white matter volume in 2 subcortical regions (parietal part of insula and transverse temporal gyrus) and in the brainstem.

Tractometry

Table 5 and Figure 2 present statistically significant differences in diffusion parameters across 32 white matter

tracts between the patient group and the healthy control group.

In patients with TLE, decreased FA was observed not only in tracts directly associated with the temporal lobe (parahippocampal, uncinate, inferior longitudinal, and arcuate fasciculi) but also in anatomically distant structures (dorsal part of the superior longitudinal fasciculus, inferior cerebellar peduncle). Ipsilateral to the seizure focus, increased RD was observed alongside decreased FA in the parahippocampal and uncinate fasciculi. Decreased FA, MD, and AD were recorded in the ipsilateral inferior cerebellar peduncle. Additionally, on the ipsilateral side, increased AD was noted in the ventral part of the superior longitudinal fasciculus, while decreased AD was observed in the inferior longitudinal fasciculus. On the contralateral side, increased AD was detected in the dorsal part of the superior longitudinal fasciculus, decreased FA in the arcuate fasciculus and inferior cerebellar peduncle, and increased RD in the dorsal part of the superior longitudinal fasciculus (Table 5).

Results comparing diffusion parameters between TLE patient subgroups – those with hippocampal sclerosis, other structural (non-hippocampal) abnormalities, drug resistance, and bitemporal discharges – are presented in Table 6.

In patients with structural abnormalities, the following changes were detected: ipsilateral increase in AD in the uncinate fasciculus and forceps minor of the corpus callosum, along with contralateral decrease in FA in the ventral part of the superior longitudinal fasciculus. In hippocampal sclerosis, contralateral reduction in AD was observed in the central part of the superior longitudinal fasciculus.

In patients with bitemporal discharges, ipsilateral increase in FA and decrease in RD in the fronto-parahippocampal tract, as well as reduced FA in the inferior longitudinal fasciculus, were identified. Additionally, this group exhibited contralateral changes in AD in the frontoparietal fasciculus.

Drug-resistant epilepsy was associated with decreased AD in the fronto-parahippocampal tract.

Discussion

Voxel-based morphometry revealed widespread changes in gray and white matter volume. These changes were observed both ipsilaterally and contralaterally relative to the primary epileptogenic focus. Volume reduction involved not only the cortex and adjacent white matter but also deep structures, including the basal ganglia, ventral forebrain regions, thalamus, and brainstem. In patients with structural abnormalities (hippocampal sclerosis or other structural non-hippocampal changes), gray matter volume reduction was noted in the ventral forebrain. Similar changes in this region were also observed in patients with drug-resistant TLE, likely explained by the higher frequency of drug resistance specifically in the structural epilepsy subgroup.

Our findings align with conclusions from previous morphometric studies in TLE. S.S. Keller et al., analyzing 18 studies, demonstrated that patients with TLE exhibit significant

Table 4. Regions of interest (ROIs) in gray matter and white matter showing differences in morphometric parameters between subgroups of patients with TLE and the group of healthy controls, Me [Q₁; Q₃]

Subgroup	Brain structures	Main group	Comparison group	p
Ipsilateral side				
Gray matter				
Hippocampal sclerosis	Thalamus	4.72 [4.16; 5.07]	5.20 [5.05; 5.45]	0.050
	Ventral forebrain	0.90 [0.82; 0.97]	0.99 [0.93; 1.10]	0.014
	Ventral forebrain	0.93 [0.82; 0.99]	1.02 [0.94; 1.25]	0.024
Structural (non-hippocampal) abnormalities	Anterior cingulate gyrus	3.74 [3.06; 4.20]*	3.04 [2.04; 3.78]	0.035
	Middle temporal gyrus	12.76 [11.05; 13.64]*	11.43 [9.64; 11.94]	0.044
	Subcallosal area	1.47 [1.33; 1.62]*	1.31 [1.00; 1.44]	0.035
Drug resistance	Ventral forebrain	0.92 [0.83; 0.98]	1.00 [0.94; 1.25]	0.018
White matter				
Hippocampal sclerosis	Parahippocampal gyrus	0.37 [0.29; 0.55]	0.50 [0.44; 0.56]	0.050
	Temporal plane	0.23 [0.14; 0.31]*	0.14 [0.10; 0.20]	0.027
Structural (non-hippocampal) abnormalities	Anterior insula	0.22 [0.19; 0.28]*	0.29 [0.20; 0.34]	0.049
	Medial segment of superior frontal gyrus	0.74 [0.68; 0.82]	0.85 [0.78; 0.99]	0.021
Drugresistance	Medial segment of the postcentral gyrus	0.11 [0.10; 0.13]	0.15 [0.12; 0.19]	0.016
	Medial segment of superior frontal gyrus	0.35 [0.33; 0.39]	0.42 [0.35; 0.50]	0.046
Bitemporal discharges	Parietal operculum	0.25 [0.24; 0.30]*	0.19 [0.16; 0.23]	0.002
	Transverse temporal gyrus	0.30 [0.24; 0.36]*	0.19 [0.11; 0.23]	0.013
	Brainstem	18.30 [17.89; 18.84]*	17.15 [15.97; 17.89]	0.036
Contralateral side				
Gray matter				
Hippocampal sclerosis	Nucleus accumbens	0.33 [0.31; 0.35]	0.38 [0.36; 0.39]	0.035
	Ventral forebrain	0.93 [0.86; 0.99]	1.05 [0.93; 1.28]	0.014
	Inferior temporal gyrus	12.89 [11.95; 14.19]*	10.82 [9.00; 13.06]	0.031
Structural (non-hippocampal) abnormalities	Medial frotnal cortex	1.57 [1.44; 1.70]*	1.33 [0.95; 1.58]	0.031
	Medial segment of superior frontal gyrus	5.98 [5.06; 6.72]*	5.55 [3.93; 6.08]	0.049
	Middle temporal gyrus	13.39 [11.44; 14.43]*	10.90 [9.34; 13.33]*	0.016
	Subcallosal area	1.47 [1.29; 1.58]*	1.27 [1.10; 1.43]	0.044
	Temporal pole	9.11 [8.53; 9.93]*	8.40 [7.26; 9.16]	0.044
Drug resistance	Brainstem	1.17 [1.06; 1.31]	1.54 [1.25; 1.98]	0.016
	Ventral forebrain	0.92 [0.86; 0.97]	1.01 [0.91; 1.19]	0.037
White matter				
Ipsilateral side				
Hippocampal sclerosis	Парагиппокампаьная извилина	0.37 [0.29; 0.55]	0.50 [0.44; 0.56]	0.027
	Parahippocampal gyrus	0.23 [0.14; 0.31]*	0.14 [0.10; 0.20]	0.031
Structural (non-hippocampal) abnormalities	Temporal plane	0.22 [0.19; 0.28]*	0.29 [0.20; 0.34]	0.049
	Anterior insula	0.74 [0.68; 0.82]	0.85 [0.78; 0.99]	0.021
Drug resistance	Medial segment of superior frontal gyrus	0.11 [0.10; 0.13]	0.15 [0.12; 0.19]	0.016
	Medial segment of the postcentral gyrus	0.35 [0.33; 0.39]	0.42 [0.35; 0.50]	0.046
	Medial segment of superior frontal gyrus	0.25 [0.24; 0.30]*	0.19 [0.16; 0.23]	0.002
Bitemporal discharges	Parietal insula	0.30 [0.24; 0.36]*	0.19 [0.11; 0.23]	0.013
	Transverse temporal gyrus	18.30 [17.89; 18.84]*	17.15 [15.97; 17.89]	0.036
Contralateral side				
Hippocampal sclerosis	Orbital part of inferior frontal gyrus	0.14 [0.10; 0.16]	0.23 [0.18; 0.24]	0.001
	Postcentral gyrus	2.14 [1.66; 2.30]*	1.75 [1.49; 1.98]	0.027
	White matter of cerebellum	10.36 [10.24; 10.86]	11.24 [10.72; 12.50]	0.044
Structural (non-hippocampal) abnormalities	Anterior cingulate gyrus	0.35 [0.29; 0.43]	0.45 [0.40; 0.57]	0.021
	Medial segment of superior frontal gyrus	0.40 [0.31; 0.45]	0.48 [0.42; 0.51]	0.035
Drug resistance	Brainstem	17.13 [15.97; 17.80]	18.42 [17.42; 21.46]	0.007
	Parahippocampal gyrus	0.45 [0.37; 0.54]	0.54 [0.46; 0.57]	0.046

Table 5. White matter tracts demonstrating differences in diffusion parameters in TLE patients compared to healthy controls, Me [Q₁; Q₃]

White matter tracts		Main group	Comparison group	p
Ipsilateral side				
FA	Parahippocampal tract	0.29 [0.26; 0.30]	0.32 [0.28; 0.45]	0.012
	Uncinate fasciculus	0.36 [0.34; 0.38]	0.43 [0.40; 0.49]	0
	Inferior cerebellar peduncle	0.37 [0.35; 0.38]	0.40 [0.36; 0.43]	0.009
MD	Inferior cerebellar peduncle	0.79 [0.76; 0.83]	0.82 [0.80; 0.91]	0.003
	Inferior longitudinal fasciculus	1.32 [1.27; 1.36]*	1.23 [1.17; 1.31]	0.009
AD	Ventral part of superior longitudinal fasciculus	1.12 [1.09; 1.14]	1.14 [1.11; 1.22]	0.015
	Uncinate fasciculus	1.21 [1.18; 1.23]	1.26 [1.20; 1.32]	0.009
	Inferior cerebellar peduncle	1.11 [1.07; 1.15]	1.19 [1.14; 1.36]	0
RD	Parahippocampal tract	0.81 [0.78; 0.85]*	0.74 [0.62; 0.83]	0.026
	Uncinate fasciculus	0.67 [0.65; 0.71]*	0.63 [0.59; 0.67]	0.011
Contralateral side				
FA	Arcuate fasciculus	0.42 [0.39; 0.44]	0.45 [0.43; 0.46]	0.01
	Inferior cerebellar peduncle	0.37 [0.35; 0.38]	0.38 [0.37; 0.40]	0.024
	Forceps major of corpus callosum	0.55 [0.51; 0.57]*	0.47 [0.39; 0.55]	0.023
AD	Dorsal part of superior longitudinal fasciculus	1.16 [1.14; 1.19]*	1.13 [1.11; 1.16]	0.036

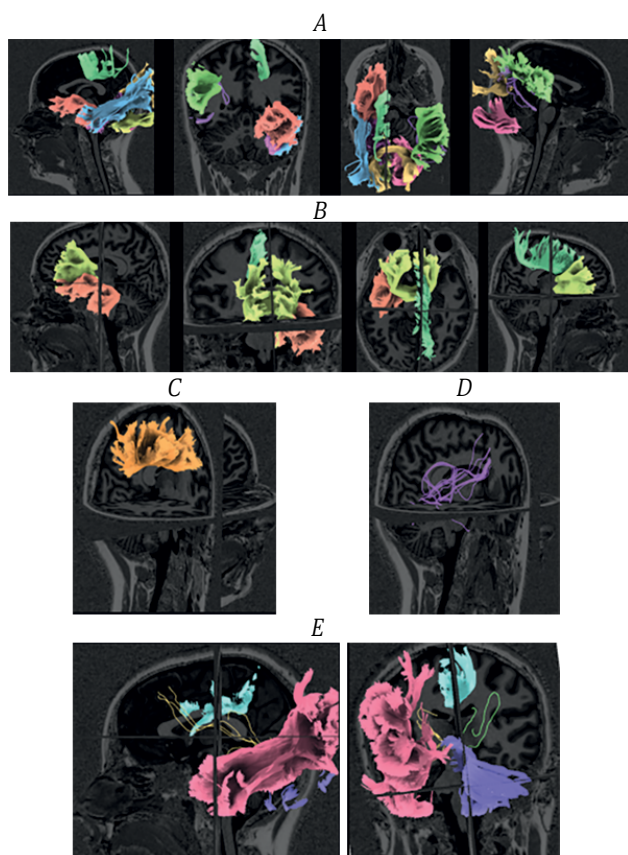


Fig. 2. White matter tracts of the brain showing differences in diffusion parameters in TLE patients compared to healthy controls. A – TLE; B – structural (non-hippocampal) abnormalities C – hippocampal sclerosis; D – drug-resistant TLE; E – patients with bitemporal epileptiform discharges.

gray and white matter brain changes. These changes affect both temporal structures (hippocampus – 82% of studies, parahippocampal gyrus – 47%, entorhinal cortex – 24%) and extratemporal regions. Among the latter, changes were most frequently described in the thalamus (ipsilaterally – 61% of studies, contralaterally – 50%), parietal lobe (47% and 53%), cingulate gyrus (41% and 35%), entorhinal cortex (24% and 6%), perirhinal cortex (12% and 0%), and fusiform gyrus (29% and 6%). The meta-analysis confirmed that structural changes are predominantly ipsilateral relative to the epileptogenic focus [6].

Increased gray matter volume in specific brain regions in patients with epilepsy may, on one hand, be attributed to structural abnormalities. Our study included patients with focal cortical dysplasia, low-grade glioneuronal tumors, encephaloceles, and cavernomas, in which congenital malformations could lead to altered gray-white matter volume ratios. On the other hand, increased gray matter volume was also detected in the cortex of the contralateral hemisphere and ventral regions of the forebrain, indicating widespread changes extending beyond the primary epileptogenic focus.

In regions with increased volume, white matter volume was significantly greater than gray matter volume. These changes were predominantly ipsilateral and mostly localized outside areas of altered gray matter. An exception was the postcentral gyrus of the contralateral hemisphere (relative to the primary epileptogenic focus), where simultaneous gray matter volume decrease and white matter volume increase were observed.

In our opinion, increased white matter volume in various, including remote, brain regions may represent the morphological substrate of the epileptogenic network.

Studies by H. Takeyama et al. and R. R. Zubal et al. report increased amygdala volume. This phenomenon is associated

Table 6. White matter tracts of the brain showing differences in diffusion parameters between subgroups of TLE patients and healthy controls, Me [Q₁; Q₃]

Subgroup	White matter tracts		Main group	Comparison group	<i>p</i>
Ipsilateral side					
Structural abnormalities	Uncinate fasciculus	AD	1.23 [1.20; 1.27]*	1.17 [1.17; 1.20]	0.005
	Forceps minor of the corpus callosum		1.35 [1.33; 1.38]*	1.30 [1.27; 1.31]	0.012
Drug resistance	Fronto-parahippocampal tract	RD	0.60 [0.57; 0.62]	0.637 [0.618–0.691]	0.026
Bitemporal discharges	Inferior longitudinal fasciculus	FA	0.42 [0.40; 0.43]	0.46 [0.43; 0.47]	0.047
	Fronto-parahippocampal tract	FA	0.46 [0.43; 0.47]*	0.41 [0.37; 0.44]	0.022
		RD	0.57 [0.54; 0.62]	0.62 [0.60; 0.66]	0.033
Contralateral side					
Hippocampal sclerosis	Central part of the superior longitudinal fasciculus	AD	1.13 [1.10; 1.17]	0.59 [0.57; 0.64]	0.047
Structural (non-hippocampal) abnormalities	Ventral part of superior longitudinal fasciculus	FA	0.37 [0.37; 0.41]	0.42 [0.40; 0.43]	0.041
Drug resistance	Fronto-parahippocampal tract	AD	1.19 [1.16; 1.24]	1.23 [1.21; 1.26]	0.047
Bitemporal discharges	Fronto-parahippocampal tract	AD	1.16 [1.06; 1.21]	1.23 [1.21; 1.26]	0.012
	Frontoparietal fasciculus	AD	1.14 [1.04; 1.19]	1.24 [1.23; 1.26]	0.000
	Inferior fronto-occipital fasciculus	FA	0.42 [0.41; 0.44]	0.46 [0.43; 0.50]	0.022
	Inferior cerebellar peduncle	FA	0.34 [0.33; 0.37]*	0.37 [0.36; 0.39]	0.040

with reduced verbal memory, presence of epileptiform activity on EEG, and sclerosis of the contralateral hippocampus. According to R. Zubal et al., amygdala enlargement may reflect compensatory neuroplastic processes in response to memory impairments, as well as result from the spread of epileptiform (ictal) activity to the contralateral cerebral hemisphere. Previously, alterations in white matter microstructure were considered as potential lateralizing markers in TLE [8]. J.K. Knowles et al. demonstrated in a mouse model that recurrent epileptic seizures cause maladaptive myelination, promoting the formation of epileptogenic networks [9]. Increased oligodendrocyte and myelin content was detected in the corpus callosum of mice with absence seizures compared to healthy controls. Antiepileptic therapy prevented maladaptive myelination, while administration of trichostatin (a histone deacetylase inhibitor suppressing oligodendrogenesis and myelination) reduced seizure frequency by 35%.

Subsequently, a large-scale coordinate-based meta-analysis was conducted [10]. This approach allows integration and comparison of data from diverse neuroimaging studies by transforming peak activation coordinates into standard anatomical space (Talairach or MNI). Results from 61 studies were included in the analysis. Statistically significant gray matter volume reductions were detected in 11 brain regions, including the thalamus (dorsomedial nucleus and pulvinar nuclei), basal ganglia (putamen and caudate nucleus), superior and inferior temporal gyri, and the superior cerebellar vermis.

In this meta-analysis, unlike our study, patients were stratified by lateralization of the epileptogenic focus. With left-sided focus localization, atrophy was detected ipsilaterally

in the cerebellar flocculus, superior temporal gyrus, and middle frontal gyrus; contralaterally – in the thalamus (dorsomedial and anterior nuclei), caudate nucleus, and cingulate gyrus. With right-sided focus, atrophy was noted in the hippocampus, parahippocampal gyrus, dorsomedial and lateral ventral nuclei of the thalamus, pulvinar nuclei, as well as in the caudate nucleus and superior temporal gyrus.

In patients with hippocampal sclerosis, according to J.M. Towne et al., ipsilateral changes were observed in the superior temporal gyrus, superior part of the cerebellar vermis, putamen, caudate nucleus, dorsomedial nucleus, and pulvinar nuclei [10]. In our study, atrophic changes in the cerebellar vermis, thalamic volume reduction, and widespread changes in the temporal cortex were also detected. However, whereas in the study by J.M. Towne et al., involvement of the basal medial nucleus of the thalamus was revealed in all cases, in our study the most significant volume reduction was noted in the ventral part of the forebrain. This structure was not separately mentioned among the most frequent findings in the cited systematic review [10].

In 2020, the international ENIGMA consortium presented results from a large-scale retrospective multicenter study examining microstructural white matter changes across various epileptic syndromes. The study analyzed diffusion tensor imaging data from 1,249 patients and 1,069 healthy controls. Patients with all forms of epilepsy exhibited decreased FA and increased MD and RD values. FA reduction was observed bilaterally in commissural, associative, and projection fibers of white matter. The most significant white matter microstructural changes occurred ipsilateral

to the epileptogenic zone in patients with focal TLE, with greater severity in cases associated with hippocampal sclerosis compared to MRI-negative forms. In patients with extratemporal seizure foci, abnormalities extended to frontocentral regions, body and genu of corpus callosum, external capsule, cingulate gyrus, and anterior corona radiata [11].

R. Mito et al. demonstrated that white matter alterations spatially correspond to structural epileptic foci locations such as hippocampal sclerosis and periventricular nodular heterotopia [12]. The authors emphasize that FA analysis enables high-accuracy lateralization of the epileptogenic zone [12], for which machine learning algorithms are currently being developed [13]. Conversely, our study also revealed significant ipsilateral diffusion parameter changes in TLE patients, though patients with structural epilepsy exhibited a distinct pattern characterized by predominant contralateral alterations.

The observed FA reduction and RD elevation across ipsilateral and contralateral hemispheric tracts in TLE patients align with earlier research findings. These changes indicate compromised microstructural integrity of white matter and likely result from prolonged exposure to epileptiform activity.

At the same time, our data indicate activation of neuroplastic processes and possible maladaptive myelination. These include:

- Increased FA and decreased RD in the ipsilateral fronto-parahippocampal bundle in patients with bitemporal discharges;
- Increased AD in the contralateral cerebellar peduncle in patients with bitemporal discharges;
- Increased AD in the contralateral cerebellar peduncle in patients with bitemporal discharges;
- Decreased MD in the inferior cerebellar peduncle in patients with TLE;

- Decreased AD in the contralateral fronto-parahippocampal and fronto-parietal bundles, as well as in the central portion of the superior longitudinal fasciculus in patients with bitemporal discharges, drug resistance, and hippocampal sclerosis.

Testing this hypothesis should be the aim of subsequent studies.

This study has several limitations. The most significant is the small sample size. This limited the applicability of parametric statistical analysis methods and may have hindered the detection of morphometric and microstructural white matter changes described in larger studies that are significant for modeling epileptogenic networks. Additionally, the automated MRI segmentation software used in the study imposes constraints on morphometric analysis. It allows assessment only of the total white matter volume of the cerebral hemispheres, cerebellum, and some superficial structures. Meanwhile, analysis of deep white matter changes in the cerebral hemispheres and assessment of white matter volume within individual brain lobes are not feasible with this methodology. Our study analyzed diffusion parameters averaged across entire tracts for selected white matter pathways. A promising area for future research is the evaluation of morphometric parameters in deep white matter regions and microstructural characteristics at key points along tracts. The selection of these points should be based on integrating clinical-anamnestic and neuroimaging data.

Conclusion

The TLE pathogenesis is characterized not only by degenerative changes in gray and white matter but also by simultaneous activation of compensatory neuroplastic mechanisms. It is the dynamic interaction and balance of these opposing processes that determine the architecture, formation, and stability of pathological epileptogenic networks.

References | Список источников

- Hainc N, McAndrews MP, Valiante T, et al. Imaging in medically refractory epilepsy at 3 Tesla: a 13-year tertiary adult epilepsy center experience. *Insights Imaging*. 2022;13(1):99. doi: 10.1186/s13244-022-01236-1
- Helmstaedter C, Al-Haj Mustafa S, Witt JA. Temporal trends indicate an epidemiological shift in the pathology of mesial temporal lobe epilepsy. *J Neurol*. 2025;272(10):652. doi: 10.1007/s00415-025-13398-1
- Wang ZI, Alexopoulos AV, Jones SE, et al. The pathology of magnetic-resonance-imaging-negative epilepsy. *Mod Pathol*. 2013;26(8):1051–1058. doi: 10.1038/modpathol.2013.52
- Télez-Zenteno JF, Hernández Ronquillo L, Moien-Afshari F, Wiebe S. Surgical outcomes in lesional and non-lesional epilepsy: a systematic review and meta-analysis. *Epilepsy Res*. 2010;89(2-3):310–318. doi: 10.1016/j.eplepsyres.2010.02.007
- Yeh FC, Panesar S, Fernandes D, et al. Population-averaged atlas of the macroscale human structural connectome and its network topology. *Neuroimage*. 2018; 178:57–68. doi: 10.1016/j.neuroimage.2018.05.027
- Keller SS, Roberts N. Voxel-based morphometry of temporal lobe epilepsy: an introduction and review of the literature. *Epilepsia*. 2008;49(5):741–757. doi: 10.1111/j.1528-1167.2007.01485.x
- Takeyama H, Matsumoto R, Usami K, et al. Late-onset temporal lobe epilepsy: enlarged amygdala-hippocampus indicates interictal epileptic activity at electroencephalography and memory impairment. *Epileptic Disord*. 2025;27(5):927–940. doi: 10.1002/epd.270061
- Zubal R, Velicky Buecheler M, Sone D, et al. Brain hypertrophy in patients with mesial temporal lobe epilepsy with hippocampal sclerosis and its clinical correlates. *Neurology*. 2025;104(2):e210182. doi: 10.1212/WNL.00000000000210182
- Knowles JK, Xu H, Soane C, et al. Maladaptive myelination promotes generalized epilepsy progression. *Nat Neurosci*. 2022;25(5):596–606. doi: 10.1038/s41593-022-01052-2
- Towne JM, Lami V, Barron DS, et al. Neuroimaging signatures of mesial temporal lobe epilepsy: a coordinate-based meta-analysis of structural and resting-state functional imaging literature. *Neuroimage Clin*. 2025;48:103908. doi: 10.1016/j.nicl.2025.103908
- Hatton SN, Huynh KH, Bonilha L, et al. White matter abnormalities across different epilepsy syndromes in adults: an ENIGMA-Epilepsy study. *Brain*. 2020;143(8):2454–2473. doi: 10.1093/brain/awaa200
- Mito R, Pedersen M, Pardoe H, et al. Exploring individual fixel-based white matter abnormalities in epilepsy. *Brain Commun*. 2023;6(1):fcad352. doi: 10.1093/braincomms/fcad352
- Sone D, Sato N, Shigemoto Y, et al. Estimated disease progression trajectory of white matter disruption in unilateral temporal lobe epilepsy: a data-driven machine learning approach. *Brain Sci*. 2024;14(10):992. doi: 10.3390/brainsci14100992

Information about the authors

Marina Yu. Maximova – Dr. Sci. (Med.), Professor, Head, 2nd Neurological department, Institute of Clinical and Preventive Neurology, Russian Center of Neurology and Neurosciences, Moscow, Russia, <https://orcid.org/0000-0002-7682-6672>

Anna D. Shitova – postgraduate student, 2nd Neurological department, Institute of Clinical and Preventive Neurology, Russian Center of Neurology and Neurosciences, Moscow, Russia, <https://orcid.org/0000-0003-0787-6251>

Marina V. Krotchenkova – Dr. Sci. (Med), Head, Radiology department, Institute of Clinical and Preventive Neurology, Russian Center of Neurology and Neurosciences, Moscow, Russia, <https://orcid.org/0000-0003-3820-4554>

Anastasia N. Sergeeva – Cand. Sci. (Med.), researcher, Radiology department, Institute of Clinical and Preventive Neurology, Russian Center of Neurology and Neurosciences, Moscow, Russia, <https://orcid.org/0000-0002-2481-4565>

Author contribution: *Maximova M.Yu.* – study conceptualization, data analysis, writing the text of the article, scientific editing; *Shitova A.D.* – conducting research, data analysis, writing the text of the article; *Krotchenkova M.V.* – study conceptualization; *Sergeeva A.N.* – development of methodology, data analysis. All authors made a final approval of the version to be published.

Информация об авторах

Максимова Марина Юрьевна – д-р мед. наук, профессор, зав. 2-м неврологическим отделением Института клинической и профилактической неврологии Российского центра неврологии и нейронаук, Москва, Россия, <https://orcid.org/0000-0002-7682-6672>

Шитова Анна Денисовна – аспирант 2-го неврологического отделения Института клинической и профилактической неврологии Российского центра неврологии и нейронаук, Москва, Россия, <https://orcid.org/0000-0003-0787-6251>

Кротенкова Марина Викторовна – д-р мед. наук, зав. отделом лучевой диагностики Института клинической и профилактической неврологии Российского центра неврологии и нейронаук, Москва, Россия, <https://orcid.org/0000-0003-3820-4554>

Сергеева Анастасия Николаевна – канд. мед. наук, н. с. отдела лучевой диагностики Института клинической и профилактической неврологии Российского центра неврологии и нейронаук, Москва, Россия, <https://orcid.org/0000-0002-2481-4565>

Вклад авторов: *Максимова М.Ю.* – создание концепции, анализ данных, написание текста рукописи, научное редактирование; *Шитова А.Д.* – проведение исследования, анализ данных, написание текста рукописи; *Кротенкова М.В.* – создание концепции, руководство научно-исследовательской работой; *Сергеева А.Н.* – разработка методологии, анализ данных. Все авторы прочли и одобрили финальную версию перед публикацией.